STRESS ANALYSIS IN THE STRUCTURE OF A TRACTOR SEAT BY USING NUMERICAL SIMULATIONS

Carlos Henrique Lara
Federal University of Lavras (UFLA), Agricultural Engineering Department, Campus, P. O. Box 3037, ZIP Code 37,200-000, Lavras, MG, Brazil
Corresponding author: chlavrasmg@gmail.com

Ricardo Rodrigues Magalhães
Federal University of Lavras (UFLA), Agricultural Engineering Department, Campus, P. O. Box 3037, ZIP Code 37,200-000, Lavras, MG, Brazil

Fábio Lúcio Santos
Federal University of Lavras (UFLA), Mechanical Engineering Department, Campus, P. O. Box 3037, ZIP Code 37,200-000, Lavras, MG, Brazil

Carlos Ademir Silva
Federal University of Lavras (UFLA), Agricultural Engineering Department, Campus, P. O. Box 3037, ZIP Code 37,200-000, Lavras, MG, Brazil

Ednilton Tavares de Andrade
Federal University of Lavras (UFLA), Agricultural Engineering Department, Campus, P. O. Box 3037, ZIP Code 37,200-000, Lavras, MG, Brazil

Abstract: Accidents involving children during the operation of agricultural machinery in unusual situations (disregarding child labor) without the responsible authorization has increased around the world. For this reason, it is needed the development of new devices to reduce the accidents risk. Based on that, this work is aimed to perform static structural analysis on the tractor seat in order to understand the von Mises stress distribution and to indicate an appropriated place to install a safety device to reduce the risk of accidents, preventing children to start tractors and then to carry out some type of operation. In this case, the tractor will only be started if the load exerted by the operator's weight on the seat is greater than the average weight of a child. For this, a unidirectional strain gage was installed in the place of the greatest stress of von Mises in the tractor seat in order to validate the simulation results. The experimental stress values results were compared with the stress values obtained in the simulation, generating a satisfactory average difference of 11.4% with a linear correlation coefficient (R^2) of 0.9997. This way, the simulations results in the tractor seat, when subjected to external loads, allowed understanding the stresses distribution in the structure and indicated an appropriated place for the installation of the safety device (region of the greatest stress in the seat) in order to avoid work accidents with children weighing under to 415.8 N.

Index terms: Work accident; safety device; strain gage; stress of von Mises.

Received: October 28, 2022 - Accepted: October 31, 2022

INTRODUCTION

The growing population expansion in the last decades ended up generating a greater demand for food, and it is therefore necessary to increase agricultural productivity to supply this demand. As a consequence, rural producers need to purchase agricultural machinery to reduce physical efforts during the tasks execution in order to increase productivity and reduce operating costs. However, operating farm equipment is one of the leading causes of farm-related injuries and fatalities among children and adolescents (Toussaint et al., 2017).

Tractor and operator represent an integrated production unit during the machine operation. Meantime the operator is exposed to high physical and mental efforts, which can result in lower productivity, decrease work quality and also increase errors and accidents (Peripolli et al., 2017).

Brazilian Regulatory Norm nº. 31 (NR 31) aims to establish the precepts to be observed in the organization and in the work environment, in order to plan and develop the agricultural activities, livestock, forestry and aquaculture compatible with safety and health in the work environment. Brazilian Regulatory Norm nº. 12 (NR 12) detailed the issue of commitment to the safety issue at work, especially labor with agricultural machinery. This Regulatory Standard and its annexes define technical references, fundamental principles and protective measurement to guarantee the health and physical integrity of workers and establish the minimum requirements for accidents and illnesses prevention at work. Both standards do not regulate child labor and prohibit this activity.

The occurrence of accidents indicates that it needs to be investigated and analyzed to find the root cause of the problem and to define the most appropriated preventive measurements for controlling operational risks (Montemor et al., 2015).

When analyzing the work evolution in the Brazilian agricultural environment, the existence of occupational risks has always been noted, but these risks were intensified and worsen since 1940´s, where the countless transformations have affected the agricultural work environment causing accidents increase (Drebes et al., 2014).

Pate and Görücü (2020) presented data about 69 fatal accidents involving young people related to the agricultural sector in the state of Pennsylvania in the United States during the period from 2000 to 2018 and concluded that 74% of fatalities happened to children older than 5. Toussaint et al. (2017) analyzed data about accidents in the agricultural sector involving 505 children and adolescents from 9 states in the Midwest of the United States from 2005 to 2010, and concluded that 307 accidents occurred with children operating agricultural machinery.

According to Wright et al. (2013) every three days a child dies in the United States due to accidents in the agricultural sector and every day 45 children are injured. The most common non-fatal injury occurred among young people aged from 10 to 15 years old, being the main sources of injury structures and surfaces, animals and agricultural machinery. Tractor injuries account for a third of all deaths (Wright et al., 2013).

Gorucu et al. (2015) analyzed 82 fatal accidents of children under 20 years old in the Pennsylvania State in the United States during the period 2000 to 2012 and concluded that children under 5 years old had the highest fatality rate of 87.1 fatalities per 100,000 farm household child per year.

From 2005 to 2014, 68% of fatal accidents involving children in the agricultural sector in Ireland were associated with the use of tractors and agricultural machinery (Health and Safety Authority, 2015). It is indicated that children under 12 years never operate tractors and that the keys are removed from the ignition and kept out of the reach of children (Health and Safety Authority, 2015). Although regulatory standards prohibit child labor, the keys must be removed from the ignition to avoid unusual situations in which children without the authorization of those responsible have the possibility of accessing the tractor and starting the ignition to carry out some type of operation (Health and Safety Authority, 2015).

Analyzing the data presented on the occurrence of accidents with children under 12 years old operating agricultural machines in unusual situations without the authorization of those responsible and that the tractor is one of the main machines used, the development of safety device that reduces the risk of accidents is justified, preventing the tractor from being started by children and that they perform some type of operation, as they do not have adequated training for operating the tractor. Based on that, this work was performed in order to indicate a proper location for installing a safety device, considering that it is possible to reduce the risk of accidents using the operator's weight as a condition to start the tractor. For this objective, it was performed stress analysis in a tractor seat structure by the Finite Element Method (FEM).

FEM theoretical background

FEM is a result in a system of algebraic equations. Initially, it is necessary to generate meshes (model discretization) from geometries involved in the study. This process consists of subdividing the model geometry into small volumes constituted by nodes and elements. When the model is subjected to external loads, some nodes change their position, causing an elastic deformation in the model. In this research, equations of a three-dimensional system with elasticity extracted from Kwon and Bang (2000) are used.

The elastic deformation vector {ε} is determined by the nodal displacements and can be numerical calculated by using Equation 1.

$$\{\varepsilon\} = \begin{Bmatrix} \varepsilon_{xx} \\ \varepsilon_{yy} \\ \varepsilon_{zz} \\ \gamma_{xy} \\ \gamma_{yz} \\ \gamma_{xz} \end{Bmatrix} = \begin{Bmatrix} \partial_u / \partial_x \\ \partial_v / \partial_y \\ \partial_w / \partial_z \\ \partial_u / \partial_y + \partial_v / \partial_x \\ \partial_v / \partial_z + \partial_w / \partial_y \\ \partial_u / \partial_z + \partial_w / \partial_x \end{Bmatrix} \quad (1)$$

Where, u is the displacement and ε_{xx} the deformation on the x axis, v is the displacement and ε_{yy} the deformation on the y axis, w is the displacement and ε_{zz} the deformation on the z axis, γ_{xy} the shear strain on the plane (x, y), γ_{yz} the shear strain in the plane (y, z) and γ_{xz} the shear strain in the plane (x, z).

After knowing the displacements and deformations at each point, it is possible to calculate the stresses acting on the model. Assuming that the model is in the linear-elastic regime for the applied loads, it is possible to apply Hooke's law. The components of the stress tensor {σ} can be calculated from:

$$\{\sigma\} = [D]\{\varepsilon\} \quad (2)$$

Where $\{\sigma\} = \{\sigma_{xx}\sigma_{yy}\sigma_{zz}\tau_{xy}\tau_{yz}\tau_{zx}\}^T$ is the vector of component stresses σ_{xx} for normal stress on the x axis, σ_{yy} for normal stress on the yaxis, σ_{zz} for normal stress on the z axis, τ_{xy} for the shear stress in the plane (x, y), τ_{yz} for the shear stress in the plane (y, z), τ_{xz} for the shear stress in the plane (x, z) and $[D]$ is the material matrix composed of information about material properties (the modulus of elasticity and Poisson's coefficient).

When external loads are applied to nodes and elements, the model behaves according to Equation 3.

$$\{F\} = [m]\{\ddot{u}\} + [c]\{\dot{u}\} + [K]\{u\} \quad (3)$$

where $\{F\}$ is the external load vector, $[m]$ is the mass matrix, $[c]$ is the damping matrix, $[K]$ is the stiffness matrix, $\{\ddot{u}\}$ is the acceleration vector, $\{\dot{u}\}$ is the velocity vector and $\{u\}$ is the displacement vector.

By assuming a static system without damping, Equation 3 can be rewritten according to Equation 4.

$$\{F\} = [K]\{u\} \quad (4)$$

In order to validate FEM models, validation processes can be used from experimental procedures. The strain gages are used in experiments to measure the deformations in specimens, as well as to determine the mechanical properties, especially the stress-strain curve of the material (Sandí and Jiménez, 2013). The configuration of the strain gage is performed by means of the Wheatstone bridge circuits that have the function of converting the resistance variation in volts units' proportional to the applied load (Dally et al., 2010).

To use the strain gage, it is necessary to calibrate the measurement system. The calibration seeks to relate the values measured by a system of acquisition of measures and values corresponding to the quantities established by standards, under certain pre-established conditions (Dally et al., 2010).

MATERIAL AND METHODS

The research was carried out at the Mechanical Vibration Laboratory of the Engineering School at the Federal University of Lavras (UFLA), Brazil.

This work first stage consisted of the three-dimensional modelling of the tractor seat support using the commercial software Solidworks®. Subsequently, a numerical FEM simulation was performed to analyze stresses and displacements using the commercial software Ansys®, version 14.5.

In order to validate the results from the numerical simulations, experiments were performed to evaluate the seat structure displacement when subjected to the same conditions imposed during the simulations.

A unidirectional strain gage was installed at the location defined during the simulations in order to evaluate the simulation results involving von Mises stresses and to indicate a suitable location for installing the safety device. The research main stages are shown in Figure 1. To plot the results graphs, the commercial software MATLAB®, version R2016a, was used.

Geometric models' generation and numerical simulation inputs

The ECO-11SM tractor seat system manufactured by Star Seating SYS (Figure 2a) was defined as the study object. This system has a standard design that can be used in most small agricultural tractors.

In order to perform numerical simulations, it was necessary to model the seat support and springs. The modelling was performed individually for each piece in the commercial Solidworks® software by measuring the geometry of the pieces using a caliper. After modelling, the main geometric characteristics were measured in the software-generated model and compared with the physical model to identify possible errors during the modelling. In this step, no differences were identified between both models.

After parts modelling, the seat support and springs were assembled in the Solidworks® commercial software (Figure 2b). The geometry of this system was exported to the Ansys® commercial software to perform the simulations.

Mechanical properties of the seat support material were defined based on the properties of SAE 1020 steel. These properties were available in the material library of the Ansys® software.

Mechanical properties (the modulus of elasticity and Poisson's coefficient) from the spring material were defined experimentally because this information was not included in the product specifications. The experiment was performed by analyzing the springs deformation for different loads (Figure 3a).

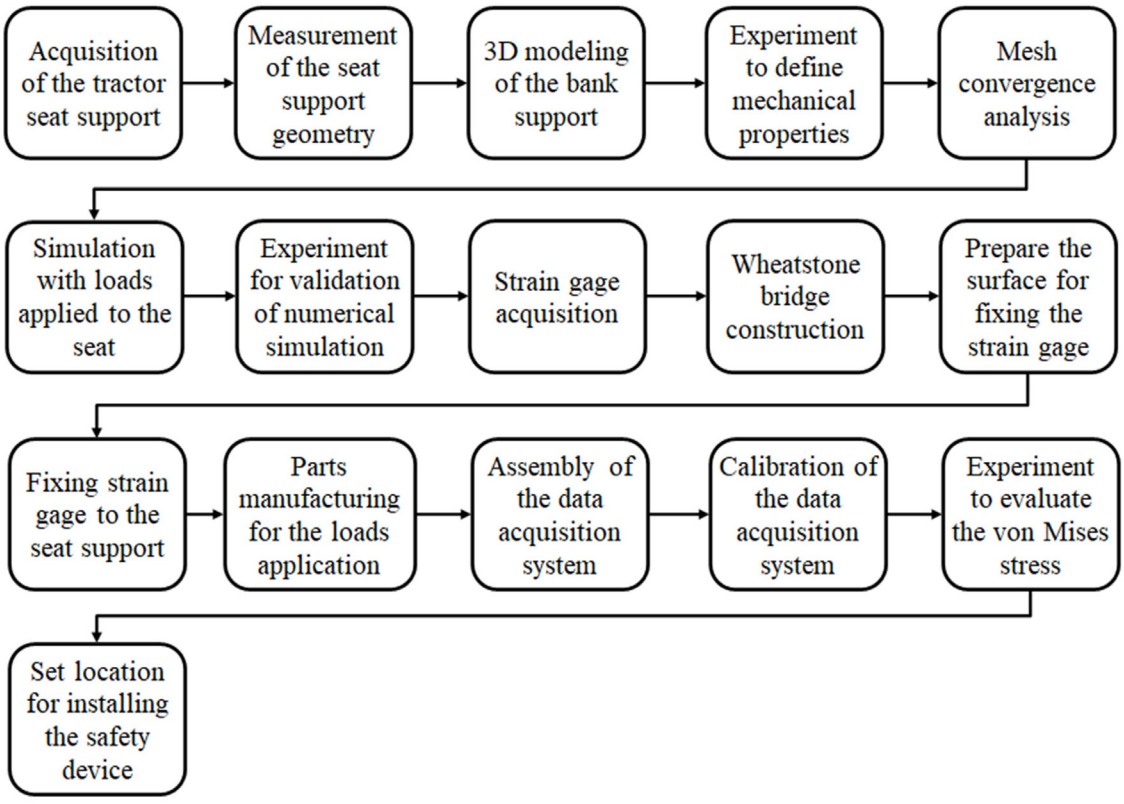

Figure 1: Main stages of the research.

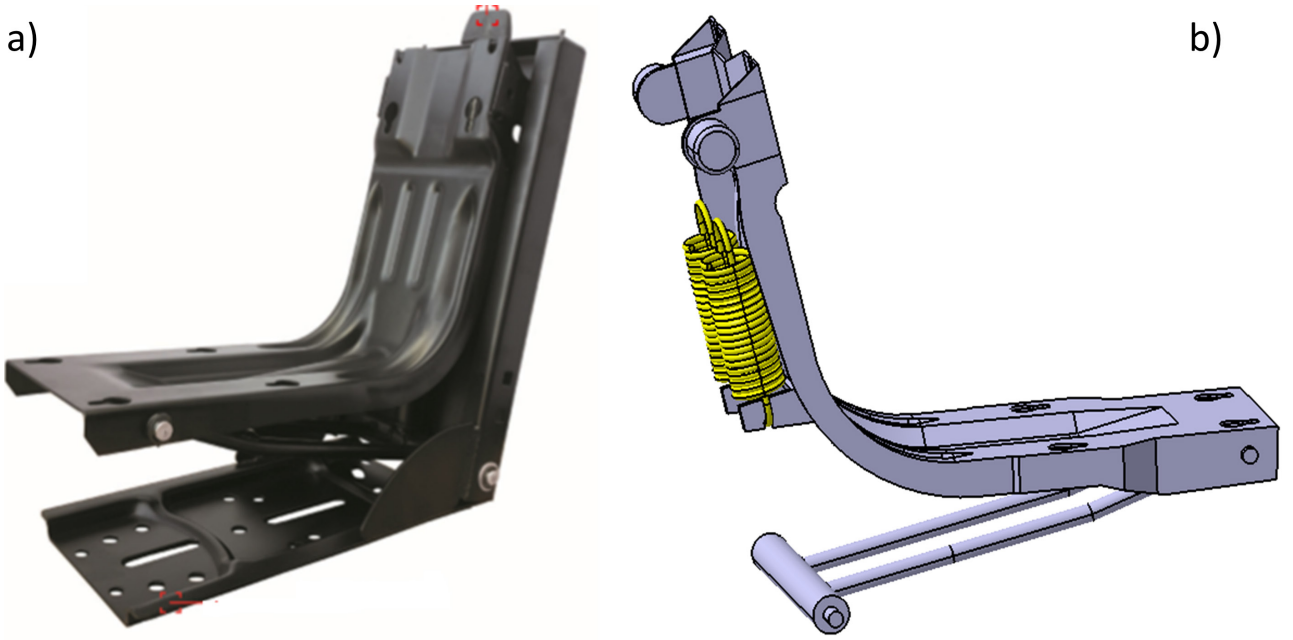

Figure 2: a) ECO-11SM tractor seat system and b) Sprung seat system.

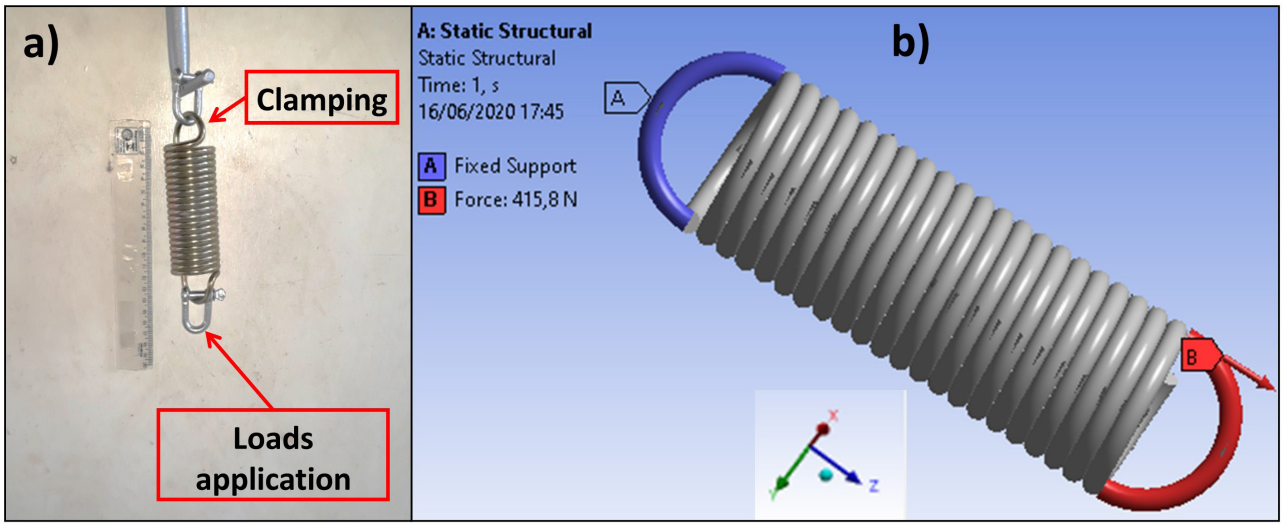

Figure 3: (a) Experiment and (b) Simulation.

Three replicates were performed with 10 deformation measurements for each spring with load variations among 156.9 N and 415.8 N. From the deformation values found it was possible to define the value of the spring constant of 8099.8 $N.m^{-1}$, according to Equation 4.

After defining the spring elastic constant, simulations were performed (Figure 3b) to define the Poisson's coefficient and elasticity modulus of the spring material. From the data obtained experimentally using a load equal to 415.8 N, spring elastic constant of 8099.8 $N.m^{-1}$ and deformation of 0.0513 m, the values of the Poisson's coefficient and elasticity modulus were tested in the simulation until the values deformation of the spring converged to the same values of deformation obtained in the experiment. Finally, Poisson's coefficient values of 0.3 and elastic modulus of 320 GPa were defined.

Mesh convergence analysis

In order to ensure simulations reliability, mesh convergence analysis was performed according to pre-established boundary conditions for the spring (Figure 3b) and for the support (Figure 4). In this analysis, a load in the seat center of 415.8 N

and two types of second-order mesh geometries (tetrahedral and hexahedral) were used for the model according to the following steps:

• Generating the mesh with the smallest number of elements as possible and generating displacements at a pre-defined point of the geometry (Figure 4) for the support;

• Refining the mesh with smaller elements and comparing the results with the previously obtained displacement values;

• Increasing the mesh density and re-analyzing the displacement results until the values stability observation.

Numerical simulation and experimental validation of the seat support displacement

To evaluate the stresses and displacements of the seat support when subjected to external loads, static structural analysis was performed. The attachment points of the seat support system were first defined as being on the two upper sides of the springs. The lower axis was fixed allowing only the set to rotate in the direction of the x axis. The support setting on the side guides was also defined, leaving only the direction of the z axis free (Figure 4). Gravitational acceleration was applied to the entire system and the loads were applied considering the operator positioned in the seat center, on the left side, on the right side and at the end (Figure 5).

According to the Brazilian Institute of Geography and Statistics (IBGE, 2008), the average weight of a twelve-year-old child in Brazil is 42.4 kg. Therefore, a load of 415.8 N (42.4 kg) was used to analyze the stresses using the von Mises criterion. Considering that this weight of 42.4 kg was used only as a reference to indicate the device installation location. The person responsible for the safety standards for the tractor operation will be able to define the load value that must be monitored according to the average weight of the authorized operators to drive the tractor.

To validate the simulation, an experiment with 3 replicates was performed with 8 measurements of support displacement when subjected to loads ranging from 215.7 N to 415.8 N. A digital caliper with 0.01 mm accuracy was used to measure the displacement of the support according to the point indicated in Figure 4. The reference used for measurement was the upper surface of the support in relation to its base, as shown in Figure 6. The mean and standard error of the displacement results obtained in the experiment were compared with the results generated through simulation with the same load configurations.

Evaluation of von Mises stress values obtained by numerical simulation

To evaluate the von Mises stress values obtained via numerical simulation in order to indicate a suitable place for the safety device installation, a unidirectional strain gage model PA-06-060BA-350-LL from the manufacturer Excel Sensors was used. The strain gage was fixed in the direction of the z axis according to the greatest stress point coordinates indicated in the simulation. The reference used for the coordinates was the center of the side guides and the support upper surface (Figure 7).

The configuration of a quarter of the Wheatstone bridge was chosen to connect the strain gage. The bridge was composed of two resistors, a potentiometer and a strain gage.

The Wheatstone bridge balance was achieved by adjusting the potentiometer until the terminal voltage for the strain gage was equal to zero. To measure this voltage, a multimeter from the Fluke manufacturer, model 115 TRUE RMS, was used.

The data acquisition system, manufactured by National Instruments, was used. This hardware was composed by NI 9237 for channel bridge input module and NI 9949 terminal accessory. The software used to communicate with the hardware was LabView® (version 16.0f2). The configuration of the hardware and software was carried out considering a quarter of the Wheatstone Bridge, as indicated in the manufacturer's manual. The data acquisition system was calibrated based on quantities established by standards, under controlled conditions.

For the application of the loads, the test machine used was the INSTRON EMIC 23-20. In addition, a load cell with a capacity of 5 kN, properly calibrated with the specific software was used.

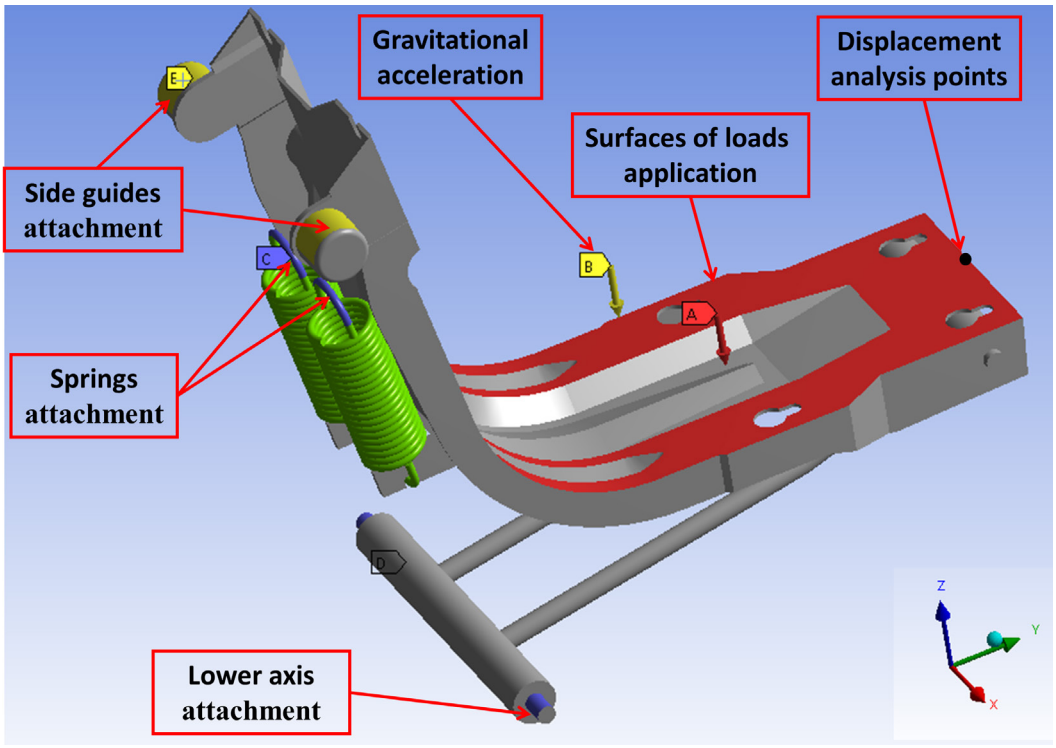

Figure 4: Set boundary conditions.

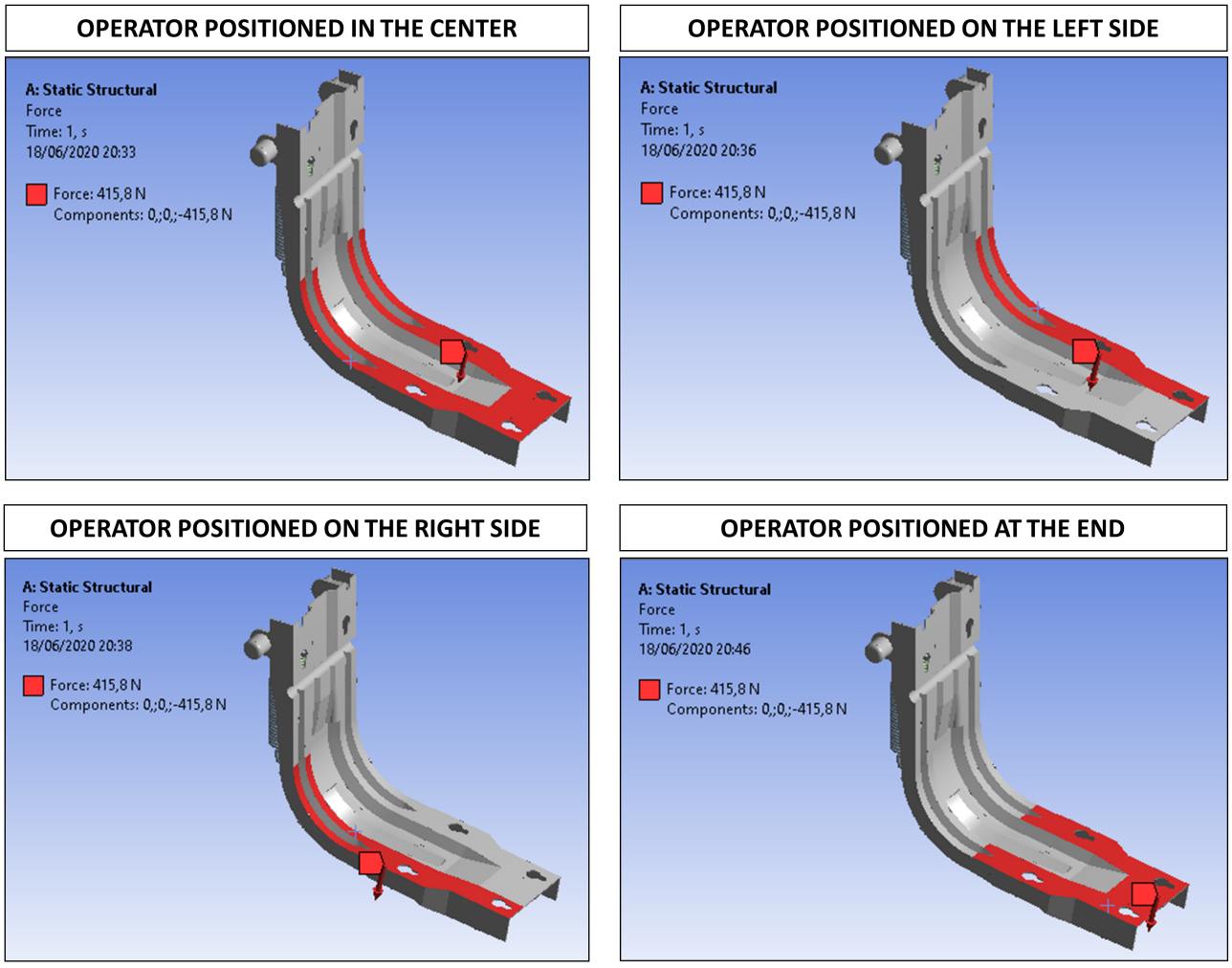

Figure 5: Place of loads application.

Figure 6: Support offset measurement reference.

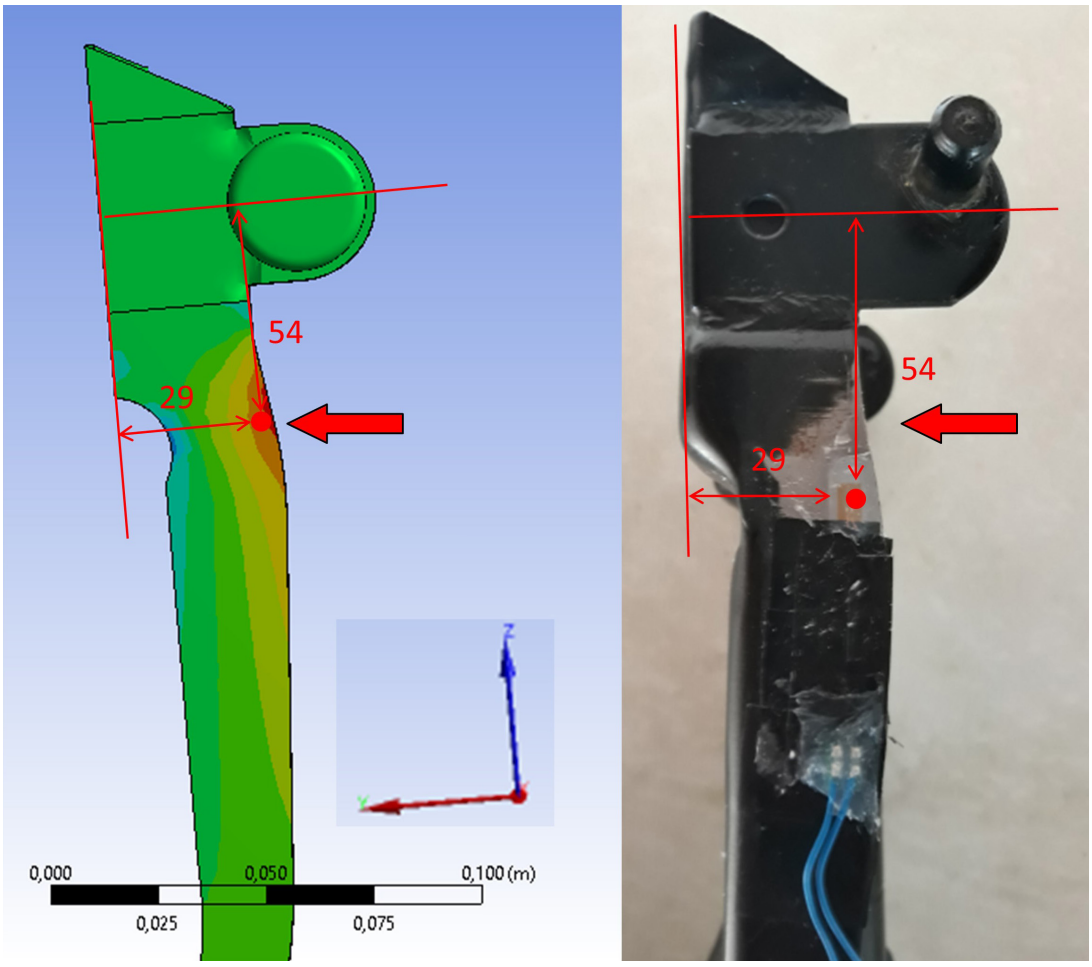

Figure 7: Location of the strain gage on the part.

The loads application location on the support was considered to be the surfaces on which the operator is positioned at the end of the seat as described in Figure 5. To simulate the same condition of loads distribution applied in the simulation, a part was made with SAE 1020 steel, 0.005 m thick and with the same geometry as the considered surfaces. The part was fixed to the support with four screws according to Figure 8. The weight of 1.06 kg of this part was considered during the loads application.

Two experiments were carried out in order to validate the stresses. The objective of the first experiment was to validate the greatest stress point indicated in the simulation, for this, the same simulation load of the 415.8 N was applied with 3 replicates and 10 stress measurements for each replica. The average stress values of the experiment was calculated and compared with the value obtained in the simulation generating a percentage of difference between them.

The second experiment objective was to generate a correlation curve between the stresses generated in the simulation and in the experiment. Thus, loads ranging from 98.1 N to 415.8 N were applied with 5 replicates and 4 stress measurements per replica. The stress values obtained in the simulation and experiment were plotted on a graph together the simple linear regression model and the experiment standard error.

RESULTS AND DISCUSSION

Simulation results to determine the spring material properties

The simulation results to determine the spring material properties are shown in Table 1.

Table 1 shows that for a Poisson's coefficient of 0.3 and a modulus elasticity of 320.0 GPa, the difference between the deformation from simulations and the one obtained from experiments was 0.88%. These values were defined as properties of the spring material and they were tested in a new simulation for loading range from 156.9 N to 415.8 N. The difference between the deformation values from the new simulations and the experiment remained 0.88%, which validated the obtained values from simulations.

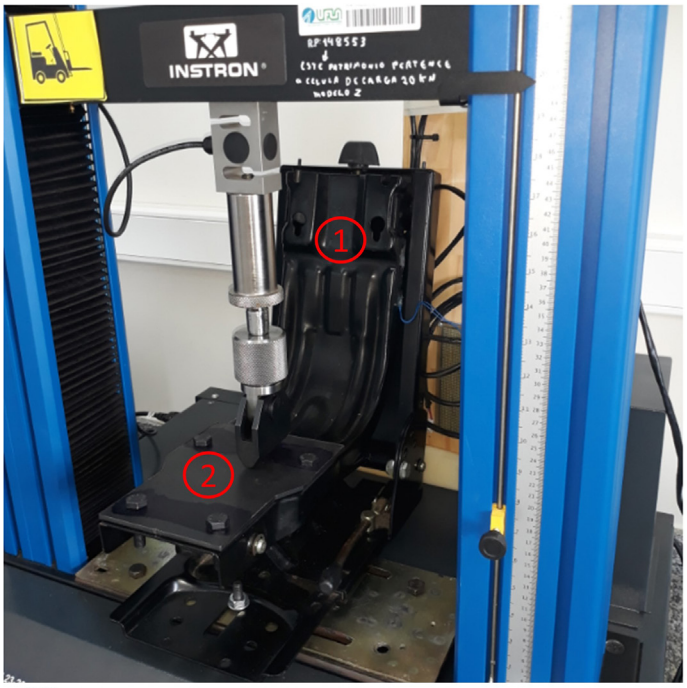

1 **Support.**
2 **Surface for application of loads.**

Figure 8: Experiment setup.

Table 1: Simulation results to determine spring material properties in Ansys® software.

Experiment data			Simulation data			Difference between experiment and simulation (%)
F (N)	K (N/m)	Deform. (m)	Poisson´s coefficient	Modulus of elasticity (GPa)	Deform. (m)	
415.8	8099.8	0.0513	0.27	210.0	0.0776	51.17%
			0.28	250.0	0.0657	27.98%
			0.29	300.0	0.0552	7.53%
			0.30	305.0	0.0547	6.56%
			0.30	310.0	0.0538	4.80%
			0.30	315.0	0.0529	3.05%
			0.30	320.0	0.0509	-0.88%

Results of mesh convergence analysis

During the analysis, it was not possible to obtain convergence of the results for the second-order hexahedral mesh. Converged results were only achieved for the second-order tetrahedral mesh for the spring and the support.

The results of mesh convergence for spring deformation were in the order of 0.0810 m for elements with dimensions between 0.004 m and 0.002 m, Figure 9. There was a reduction of 38.2% in the number of nodes and 41.7% in the number of elements with dimensions between 0.004 m and 0.002 m, that is, there was a significant reduction of 54% in the computational time during the numerical simulations. In order to reduce computational time during numerical simulations, elements with a dimension of 0.004 m were used.

The results of mesh convergence for displacement of the support were in the order of 0.0244 m for elements with dimensions among 0.004 m and 0.002 m, as shown in Figure 10. There was a reduction of 50.8% in the number of nodes and 53.5% in the number of elements with dimensions among 0.004 m and 0.002 m, that is, in this case there was also a significant reduction of 67% in the computational time during the numerical simulations. In order to reduce computational time during numerical simulations, elements with a dimension of 0.004 m were used.

Results of numerical simulation and experimental validation of the seat support displacement

The seat support displacements results obtained from numerical simulations and in the experiments are shown in Figure 11.

As noted in Figure 11, the maximum difference between the displacement values was 1.1%, considering a maximum load of 415.8 N. The simulation and experimental results showed linearity in the displacement values, i.e., when the loads on the seat support were increased by a mean of 29.4 N, the displacement increased by 0.00160 m and 0.00158 m in the simulations and the experiments, respectively.

It was also found that, with the application of the 415.8 N load considering the operator positioned in the center and at the end of the seat, the stress concentration in the entire seat support behaved symmetrically as expected (Figure 12). No stress values above the yield limit of SAE 1020 steel, which is approximately 350 MPa, were identified.

The maximum stress points were 95.1 MPa and 102.8 MPa with the operator positioned in the center and at the end of the seat, respectively. These points are located on the upper part of the seat on both sides (Figure 12) and indicate the potential local for installing a strain gage to measure deformations in the region and the development of the safety device. Considering the operator positioned on the seat left and right sides, the maximum stress points were 102.7 MPa, remaining in the upper part of the seat on the same side where the load was applied. The stress values of the x, y and z planes are detailed in Table 2.

Sindhu and Naidu (2017) analyzed the stresses in the structure of a tractor seat using numerical simulations with a force of 1000 N applied to the bottom of the structure. Authors found a maximum stress value of 107.9 MPa, which is below the yield value of the material used. The difference found from this work can be justified by the seat structure designs which were based on different concepts.

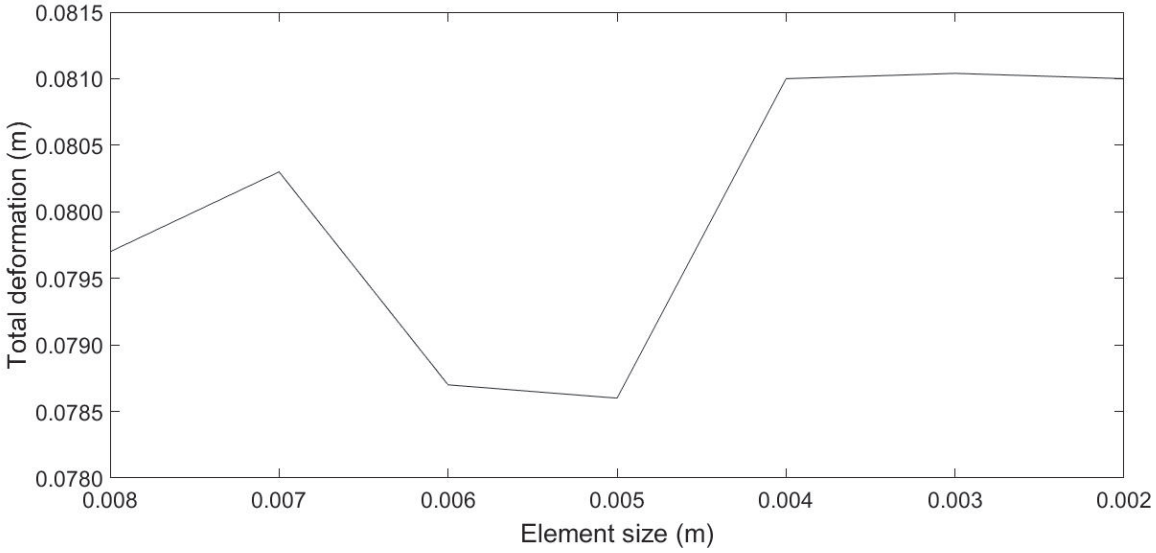

Figure 9: Convergence analysis of the spring with tetrahedral geometry mesh.

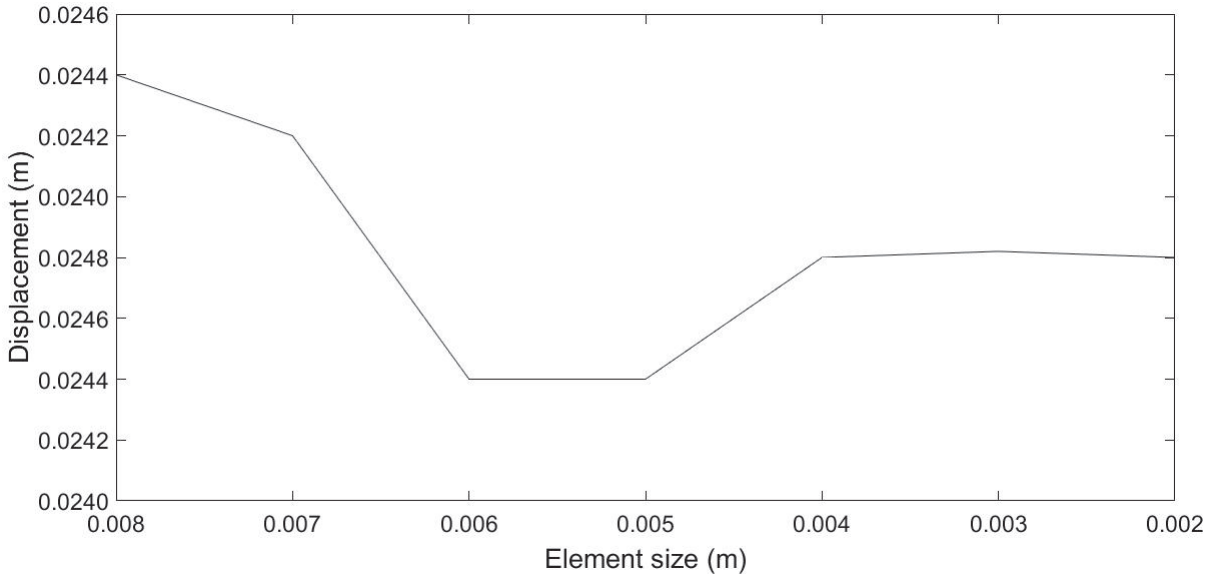

Figure 10: Convergence analysis of the support with tetrahedral geometry mesh.

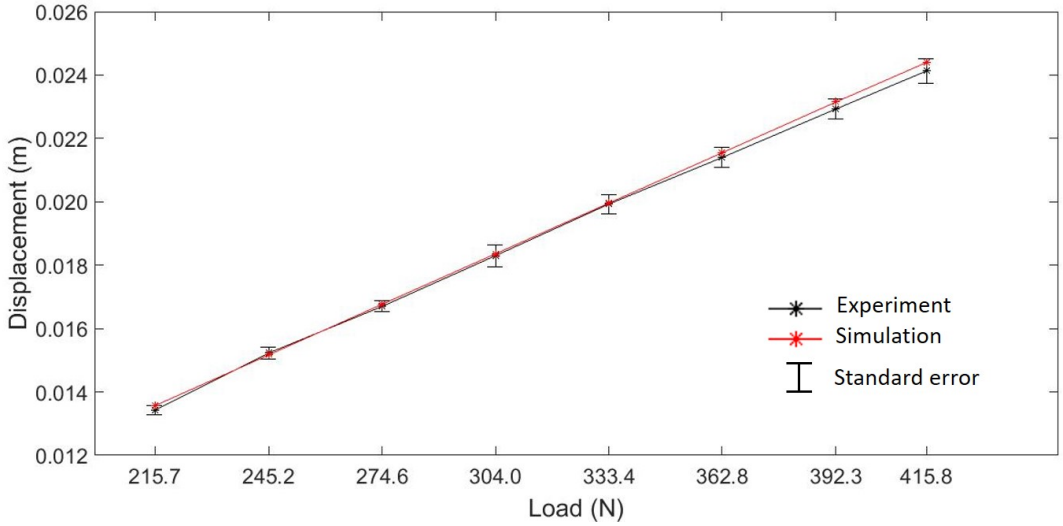

Figure 11: Results of the seat support displacements.

In addition, the tractor seat structure analyzed by Sindhu and Naidu (2017) was more robust than the structure analyzed in this study.

Results of evaluation von Mises stress values obtained by numerical simulation

The results of the stress values of the simulation and the experiment are shown in Table 3. The stress value obtained in the simulation was 105.8 MPa and the average stress of the experiment was 93.8 MPa, generating a difference of only 11.4%. Yurdem et al. (2019) performed a numerical simulation via FEM on a moldboard plough to determine the points of the greatest von Mises stress concentration at various points in the plough structure when subjected to a 20 kN load. To validate the simulation, the authors installed strain gages on the plough structure at the same points indicated in the simulation and the average difference obtained between the stress values of the simulation and experiment was 22%. Valladares et al. (2014) used computational and experimental methods in a project to optimize a semitrailer axle support subjected to fatigue loads. The results obtained via FEM for von Mises stress values were correlated with extensiometric tests in order to assess the accuracy of the computational method, obtaining a difference between the experimental stress values and in the simulation around 31%. Considering that the difference

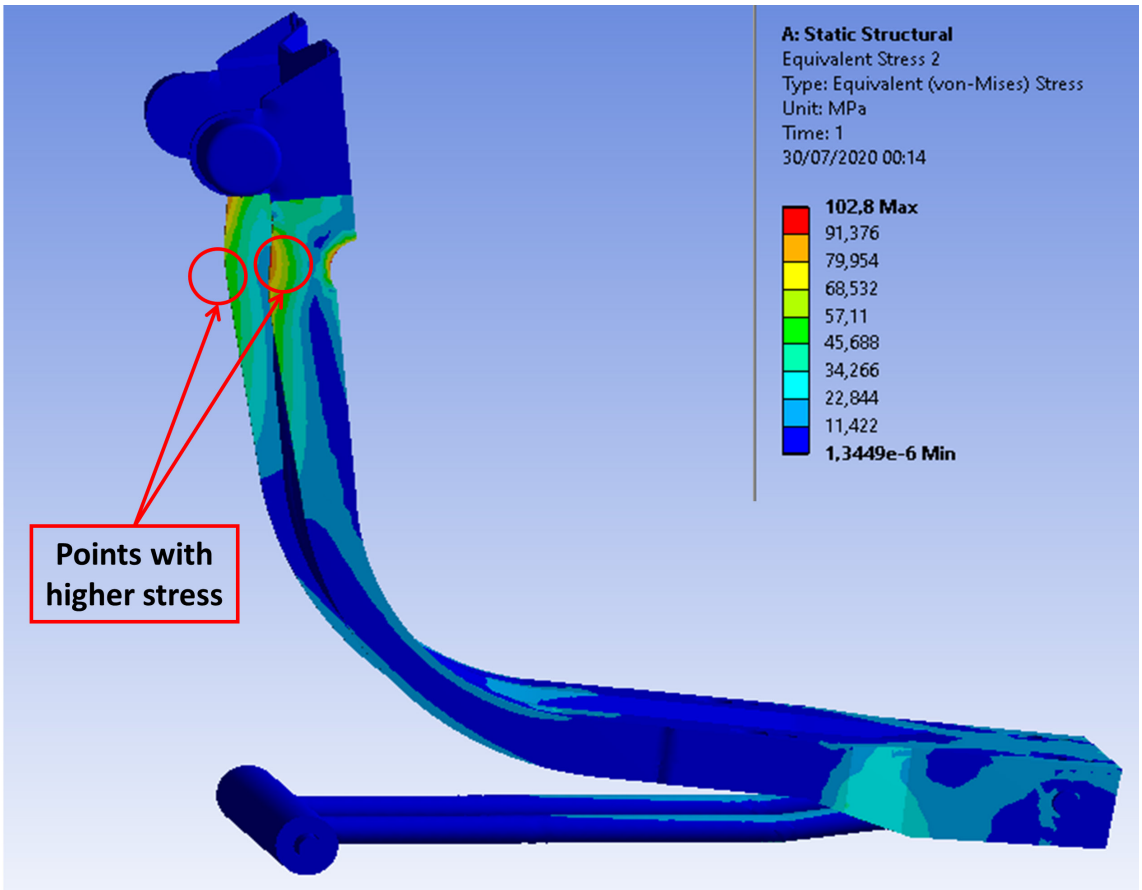

Figure 12: Results of stress analysis on seat support (operator positioned at the end).

Table 2: Von Mises stress result in the simulation.

Operator´s position in the seat	(MPa)	(MPa)	(MPa)	(MPa)
Centre	95.1	39.5	41.7	97.9
Left side	102.7	43.2	53.7	105.8
Right side	102.7	43.2	53.7	105.8
At the end	102.8	42.9	46.9	105.8

found in this study was 11.4% (Table 3), it is possible to state that the results obtained for the stress distribution in the seat support when it is subjected to external loads were adequate, when compared with data from literature.

The graph with the linear adjustment curves of the stresses obtained in the simulation and experiment is shown in Figure 13. When analyzing the stress curve of the experiment, the correlation between the data is justified by the value of the linear correlation coefficient (R^2) of 0.9997. The maximum difference found between the stress values of the experiment and simulation was 10.8% for the 196.1 N load and the minimum difference obtained was 9.3% for the 294.2 N load. These results demonstrated good repeatability among the measurements performed. Naderi et al. (2008) used strain gages to measure the dynamic load of the driving wheels of a tractor in order to improve the efficiency of traction. The values obtained through the use of strain gages in the experiment with loads ranging from 6.5 kN to 20.6 kN were compared with the values obtained through the dynamic load prediction equations. The minimum difference found among the values of the calculated dynamic load and the experiment was 9% and the maximum difference was 20%. The simple linear correlation coefficient (R^2) of the measurements made in the experiment was 0.95.

Table 3: Results of average values of stress between simulation and experiment.

Simulation data		Experiment data				
F (N)	σ (MPa)	Sample	σ (MPa) mean between replica	% difference between simulation / experiment	σ (MPa) – experiment mean	% difference between simulation / experiment
415.8	105.8	1	93.4	11.7%	93.8	11.4%
		2	93.4	11.7%		
		3	91.8	13.2%		
		4	95.1	10.1%		
		5	98.4	7.0%		
		6	90.2	14.8%		
		7	90.2	14.8%		
		8	91.8	13.2%		
		9	96.7	8.6%		
		10	96.7	8.6%		

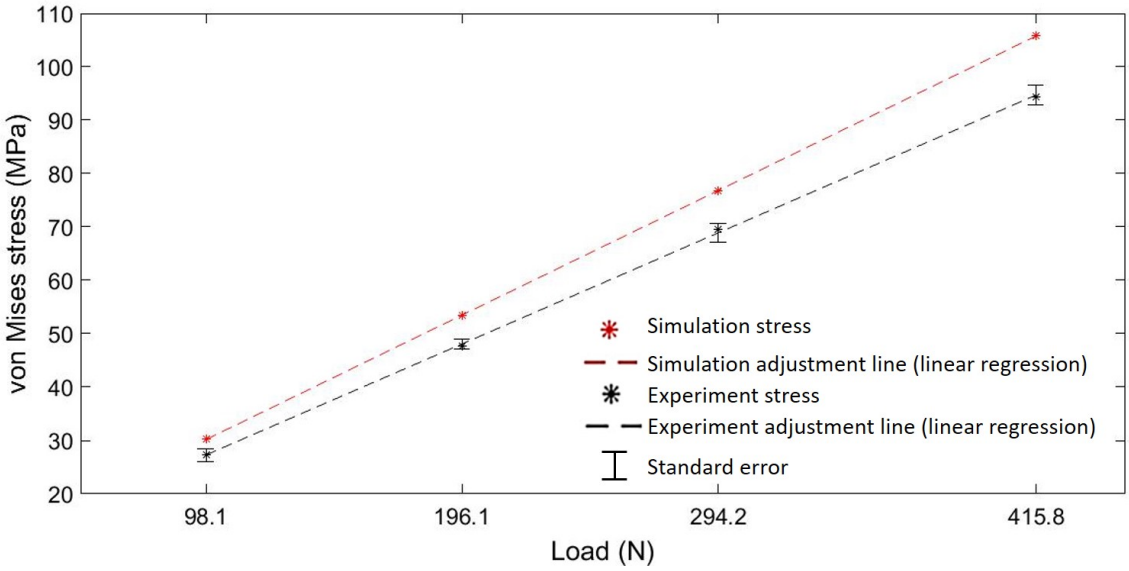

Figure 13: Stress versus load graph between simulation and experiment.

The linearity of the values obtained in the experiment shows agreement with Hooke's law for deformations within the elastic region of the material and thus allowed the validation of the proposed measurement system. The use of a potentiometer in the construction of the Wheatstone bridge made it possible to balance the bridge voltages, thus ensuring greater assertiveness in data collection.

The linearity of the values obtained in the experiment validates the location indicated in the simulation for installing the safety device. The strain gage itself can be used as a safety device as long as a communication interface with the tractor ignition system is implemented. Future researches can be developed to design this communication interface and the safety device. It is indicated that the installation of the strain gage is made on both sides of the indicated location, since the stress distribution behaved in a symmetrical manner.

The use of the strain gage for load and deformation measurements proved to be an advantageous option when presenting linearity in response to load applications. In addition, the strain gage has a low acquisition cost and can be used in several applications for measuring load and strain.

CONCLUSIONS

It was possible to understand the von Mises stress distribution from static structural analysis via FEM, when the tractor seat is subjected to external loads and also to indicate the location for the installation of the proposed safety device.

The distribution of the stress values behaved symmetrically around the tractor seat. The stress value obtained in the simulation was 105.8 MPa and the average stress of the experiment was 93.8 MPa, generating a difference of only 11.4%. The results obtained for the distribution of stress were adequated when compared with data from literature that presented differences of 22% and 31% between values of simulation and experiment.

The location indicated for installing the safety device is the point with the highest stress concentration of 105.8 MPa obtained in the numerical simulation according to Figure 20. The strain gage itself can be used as a safety device as long as a communication interface with the tractor ignition system is implemented. Future research can be carried out to develop this communication interface and the security device.

The mesh convergence analysis proposed for the model ensured the reliability of the results, in addition to providing a significant reduction in computational time of 54% during simulations with the spring and 67% in simulations with the tractor seat.

Although NR12 and NR31 standards do not child labor and prohibit this activity, it was evident that there are risks for accidents associated with unusual situations that can occur in the work environment, such as forgetting the ignition key on the tractor, thus allowing access and tractor operation can be carried out by children without authorization from the responsible person.

The use of the strain gage for load and strain measurements proved to be an advantageous option when presenting linearity in response to load applications. In addition, the strain gage has a low acquisition cost and can be used in several applications for measuring load and strain. Future researches can be developed to design the safety device and evaluate the investment with cost/benefit analysis for large scale production.

REFERENCES

BRASIL. Ministério do Trabalho e Emprego. **NR 12 – Segurança no trabalho em máquinas e equipamentos**. Brasília: Ministério do Trabalho e Emprego, 2015. <http://trabalho.gov.br/seguranca-e-saude-no-trabalho/normatizacao/normas-regulamentadoras/norma-regulamentadora-n-12-seguranca-no-trabalho-em-maquinas-e-equipamentos>.

BRASIL. Ministério do Trabalho e Emprego. **NR 31 - Segurança e saúde no trabalho na agricultura, pecuária, silvicultura, exploração florestal e aquicultura**, 2015. <https://enit.trabalho.gov.br/portal/images/Arquivos_SST/SST_NR/NR-31.pdf>.

DALLY, J. W., RILEY, W. F., MCCONNELL, K. G. **Instrumentation for Engineering Measurements. New Delhi**, India: Wiley India Private Limited, 2010.

DREBES, L. M., SCHERER, C. B., GONÇALVES, J.R., DÖRR, A.C. Typical rural work accidents: a study of records from the University Hospital Santa Maria, RS, Brazil. **Monografias Ambientais – REMOA**, 13(4):3467-3476, 2014.

GORUCU, S., MURPHY, D., KASSAB, C. Occupational and nonoccupational farm fatalities among youth for 2000 through 2012 in Pennsylvania. **Journal of Agromedicine**, 20(2):125-39, 2015.

HEALTH AND SAFETY AUTHORITY. Child tractor safety. <https://www.hsa.ie/eng/Your_Industry/Agriculture_Forestry/Young_Elderly_on_Farms/Children_on_Farms/Child_Tractor_Safety/>, 2015.

IBGE. **SIDRA**, Instituto Brasileiro de Geografia e Estatística, 2008. <https://sidra.ibge.gov.br/tabela/2657>.

KWON, Y.W., BANG, H. **The finite element method using MATLAB**. Washington, D.C., 2000: CRC press.

MONTEMOR, C., VELOSO, L., AREOSA, J. Accidents with agriculture and forestry tractors: to learn for preventing. **Revista da Faculdade de Letras da Universidade do Porto**, 30(1):119-143, 2015.

NADERI, M., ALIMARDANI, R., ABBASZADEH, R., AHMADI, H. Assessment of Dynamic Load Equations Through Drive Wheel Slip Measurement. **American-Eurasian Journal of Agricultural & Environmental Sciences**, 3(5):778-784, 2008.

PATE, M. L., GÖRÜCÜ, S. Agricultural Work-Related Fatalities to Non-Working Youth: Implications for Intervention Development. **Journal of Agricultural Safety and Health**, 26(1):31-43, 2020.

PERIPOLLI, J. L. Z., ALONÇO, A.S., POSSEBOM, G. Conformation of the internal free space of agricultural tractors and mandatory security items according to NBR/ISO 4252 and NR 12 standards. **Tecno-Lógica**, 21(2):103-107, 2017.

SANDÍ, A. M., JIMÉNEZ, A.A. Comparación de determinación de propriedades mecânicas en barras de refuerzo para concreto com extensómetro axial convencional y extensômetro láser. **Métodos y Materiales**, 3(1):4-20, 2013.

SINDHU, P., NAIDU, M. K. Experimental and Finite Element Analysis of Seat Frame and Bonnet of a Tractor. **International Journal for Research in Applied Science & Engineering Technology (IJRASET)**, 5(4):108-126, 2017.

TOUSSAINT, M., FAUST, K., PEEK-ASA, C., RAMIREZ, M. Characteristics of Farm Equipment-Related Crashes Associated with Injury in Children and Adolescents on Farm Equipment. **The Journal of Rural Health**, 33(2):127-134, 2017.

VALLADARES, D., CARRERA, M., CASTEJON, L., MARTIN, C. Application of Computational-Experimental Methods for Designing Optimized Semitrailer Axle Supports. **Sage Journals,** 4(2):1-19, 2014.

WRIGHT, S., MARLENGA, B., LEE, B. C. Childhood agricultural injuries: an update for Clinicians. **Current Problems in Pediatric and Adolescent Health Care**, 43(2):20-44, 2013.

YURDEM, H., DEGIRMENCIOGLU, A., CAKIR, E., GULSOYLU, E. Measurement of strains induced on a three-bottom moldboard plough under load and comparisons with finite element simulations. **Measurement,** 136(1):594-602, 2019.